Chinese Chemical Letters 34 (2023) 108062

Contents lists available at ScienceDirect

Chinese Chemical Letters

journal homepage: www.elsevier.com/locate/cclet

Ultralong room temperature phosphorescence *via* the charge transfer-separation-recombination mechanism based on organic small molecule doping strategy

Yanan Wang, Chao Wang, Jingran Zhang, Yurong Guo, Peng Zhao, Xiaoxue Fang, Guangjiu Zhao*

Molecular Dynamic Chemistry Center, Tianjin Key Laboratory of Molecular Optoelectronic Sciences, Department of Chemistry, School of Science, Tianjin University, Tianjin 300354, China

ARTICLE INFO

Article history:
Received 25 July 2022
Revised 19 November 2022
Accepted 12 December 2022
Available online 13 December 2022

Keywords:
Ultralong room-temperature phosphorescence
Charge transfer-separation-recombination
Organic small-molecule
Doped system
Luminescent mechanism

ABSTRACT

Ultra-long room temperature phosphorescence (URTP) has been increasingly recognized in pure organic luminophor in recent years. Through a simpler molecular design and charge separation-recombination pathway, organic luminophor can achieve even better URTP properties. In this work, we achieved URTP in a system of host-guest doped benzophenone derivatives whose phosphorescence is visible to the naked eye. The differences in the wavelength lifetimes of luminescent emission correspond to different photophysical mechanisms. Through a combination of theoretical calculations and experiments, the host acts as a powerful substrate that restricts the motion of the guest and inhibits the non-radiative transitions of the guest, accompanied by a charge transfer separation-recombination process between the host and the guest, resulting in an URTP phenomenon. Transient absorption results demonstrate the existence of a charge-separated state. The design strategy *via* charge separation is generic and easy to implement, providing a direction for the future design of doped URTP.

© 2023 Published by Elsevier B.V. on behalf of Chinese Chemical Society and Institute of Materia Medica, Chinese Academy of Medical Sciences.

Room temperature phosphorescence (RTP) has attracted extensive attention for its potential applications in biological imaging [1,2], anti-counterfeiting [3–5] and organic light-emitting diodes [6–8] due to its long luminescence lifetime and high exciton utilization. Based on traditional RTP studies, Ultra-long room temperature phosphorescence (URTP) has received a lot of attention from researchers in recent years due to its more unique photophysical processes and superior luminescence properties [9–13]. In general, the URTP characteristics of pure organic molecules in the solid state are significantly dependent on intermolecular interactions [14,15]. A variety of strong intermolecular interactions, including intermolecular hydrogen bonding, halogen bonding, and π-π stacking, can be effectively overcome the spin forbidden transition between singlet and triplet states, and achieve efficient intersystem crossing (ISC) process, which can stabilize the triplet state and promote the persistent URTP effect. Many URTP materials have been designed and developed using design strategies such as halogen bond interaction [16,17], crystallization engineering [18,19], H-aggregation [20], heavy atom effect [16,21], polymerization [22–24] and host-guest doping [2,12,15,18,25-31]. A basic and practical technique for obtaining organic afterglow materials is the construction of host-guest doped system. The following are the primary methods of thinking for host-guest doping to achieve prolonged phosphorescence at the moment. The rigid matrix efficiently inhibits the guest molecules and prevents the triplet state energy from being quenched by ambient humidity and oxygen [18,32]. Furthermore, appropriate triplet energy levels of the host matrix can also provide an effective transition path for energy transfer between the host matrix and the guest, which is conducive to the generation and stability of triplet excitons [15,33]. However, the mechanism for generating URTP is the part that differs from RTP. Here, we propose an unusual mechanism to explain the URTP phenomenon.

Currently, Ma group disclosed several new methods for achieving URTP in doped systems and made some progress [34–37]. Zhang group reported some benzophenones and derivatives as the host combined with ICT-type molecules as the guest for doping to achieve RTP [38–40]. Here, we choose 2ClBP as the host and BPTPA/BP2TPA as the guest to achieve the unique URTP. It has been reported that 2ClBP, BPTPA and BP2TPA have crystallization

* Corresponding author.
E-mail address: gjzhao@tju.edu.cn (G. Zhao).

https://doi.org/10.1016/j.cclet.2022.108062
1001-8417/© 2023 Published by Elsevier B.V. on behalf of Chinese Chemical Society and Institute of Materia Medica, Chinese Academy of Medical Sciences.

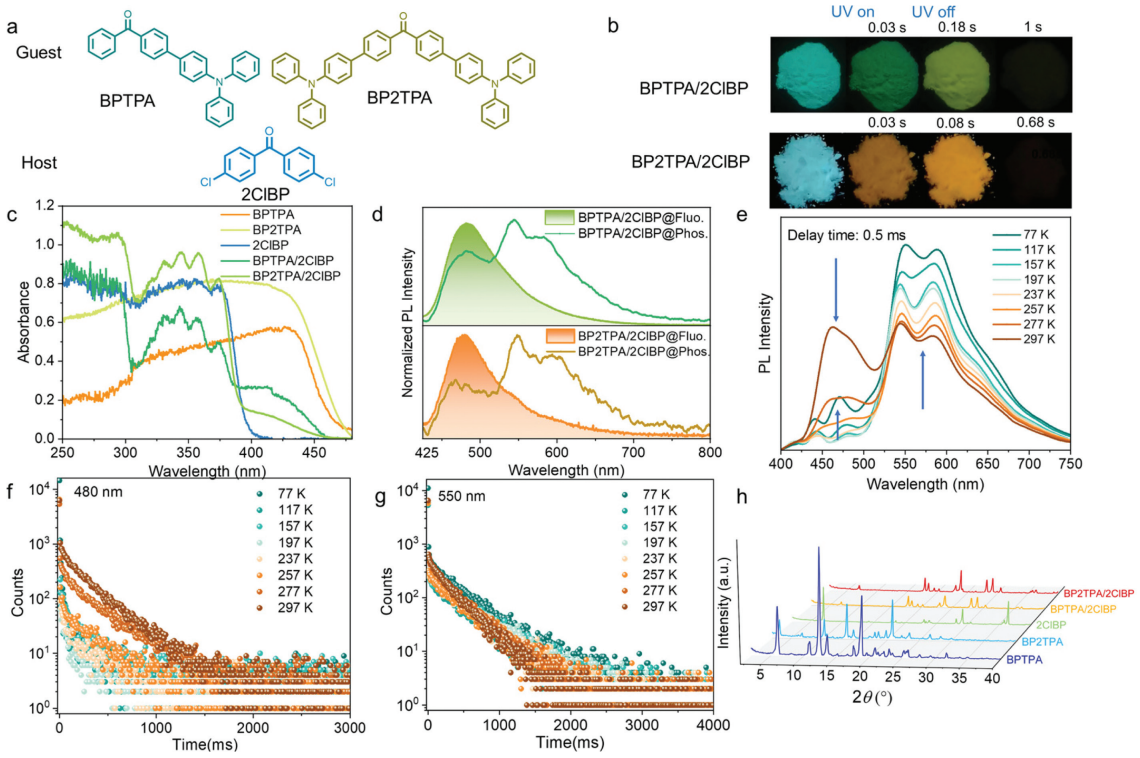

Fig. 1. (a) The molecular structures of the guest and host molecules. (b) URTP behaviors of physically mixed BPTPA/2ClBP@1:100 and BP2TPA/2ClBP@1:100 after grinding. (c) UV-vis spectra of BPTPA, 2ClBP, BP2TPA, BPTPA/2ClBP@1:100 and BP2TPA/2ClBP@1:100 (solid). (d) Fluorescence spectra (shaded part) and phosphorescence spectra (solid line) of doped systems. Excitation wavelength: 380 nm. (e) The delayed emission spectra of doped BPTPA/2ClBP@1:100 at different temperatures (delay time: 0.5 ms). Time resolved PL decay curves of BPTPA/2ClBP@1:100 at (f) 480 nm and (g) 550 nm. (g) Photoluminescence spectra of BPTPA (solid) at 77 K or room temperature. Excitation wavelength: 380 nm. (h) The XRD of BPTPA, 2ClBP, BPTPA/2ClBP@1:100 and BP2TPA/2ClBP@1:100.

induced phosphorescence/low temperature phosphorescence properties [41,42], but no URTP phenomenon can be observed. The URTP was induced by creatively combining the host and guest of this type and applying external stimuli.

Fig. 1a shows the molecular structure of host 2ClBP, guest BPTPA and BP2TPA, respectively. All three have the structure of benzophenone, which is conducive to the generation of n-π^* transition. Fig. 1b shows that the host and guest are combined by solid-state grinding. After switching off the UV lamp, the phosphorescence of the BPTPA/2ClBP@1:100 and BP2TPA/2ClBP@1:100 (molar ratio) systems were observed. There is a relationship between changes in lifetime and luminous intensity of the doped system after UV off. At the same time, the intensity change over a short period of time is related to the exposure time parameter. Fig. S1 (Supporting information) shows the URTP phenomenon at various doping ratios. It can be seen that the URTP phenomenon cannot be observed with the BPTPA, BP2TPA, and 2ClBP molecules alone. Fig. S2 (Supporting information) implies URTP can also be achieved by heating. From the UV-vis absorption spectra of host, guest molecules and doped system (Fig. 1c), the doped system has obvious host and guest characteristic peaks and wide UV absorption spectra. The liquid absorption and emission spectra of the host and guest with different solvent conditions are shown in Fig. S3 (Supporting information). The host and guest absorption are basically not affected by the solvent. In terms of emission spectra, BPTPA and BP2TPA exhibited obvious intramolecular charge transfer characteristics, and the red shift was obvious with the increase of solvent polarity [42]. Fig. 1d implicits the fluorescence/phosphorescence emission spectra of BPTPA/2ClBP@1:100 and BP2TPA/2ClBP@1:100, respectively, with excitation wavelengths of 380 nm. For the fluorescence peaks, the two doped systems are 483 nm and 476 nm, and the phosphorescence peaks are approximately 484 nm, 543 nm, 583 nm and 479 nm, 549 nm and 600 nm, respectively. Compared with BPTPA/2ClBP, BP2TPA/2ClBP has a slightly blue-shifted fluorescence spectrum and an overall slightly red-shifted phosphorescence spectrum. Approximate spectra proved relatively similar excited state properties. To clarify the attribution of different delayed emission peaks, the prompt/delayed spectra of BPTPA/2ClBP@1:100 at different temperatures were recorded (Fig. S4 in Supporting information and Fig. 1e). The delayed emission peak at 480 nm exhibits a significant decrease and then a small enhancement during the temperature change from 77 K to 297 K. Combined with the PL decay at 480 nm (Fig. 1f), we believe that the emission at 480 nm should be dominated by long delayed fluorescence. The reason for the small enhancement of emission at low temperatures and the division into two emission peaks may originate from the low-temperature phosphorescence of 2ClBP [41]. It can be seen that the delayed emission spectra and lifetimes at 550 nm as well as 600 nm exhibit distinct phosphorescence emission characteristics (Fig. 1g and Fig. S5 in Supporting information). The PL decay curves of BP2TPA/2ClBP at room temperature are shown in Fig. S6 (Supporting information). And Fig. S7 (Supporting information) shows the PL emission spectra of the guest in the solid and solution states. The phosphorescence spectra of guest at 77 K are similar to the doped system. Fig. S8 (Supporting information) shows the solid-state fluorescence emission of the host, guest and doped system. The emission position after doping is closer to the emission peak position of the guest. The XRD of the host and guest (Unground) systems, as well as the doped system, revealed that no new peak was produced after doping (Fig. 1h). And it was similar to XRD of the host. It was assumed that doping had no effect on the crystal structure of the host. Fig. S9 (Supporting information) shows the guest BPTPA aggregation-induced emission (AIE)

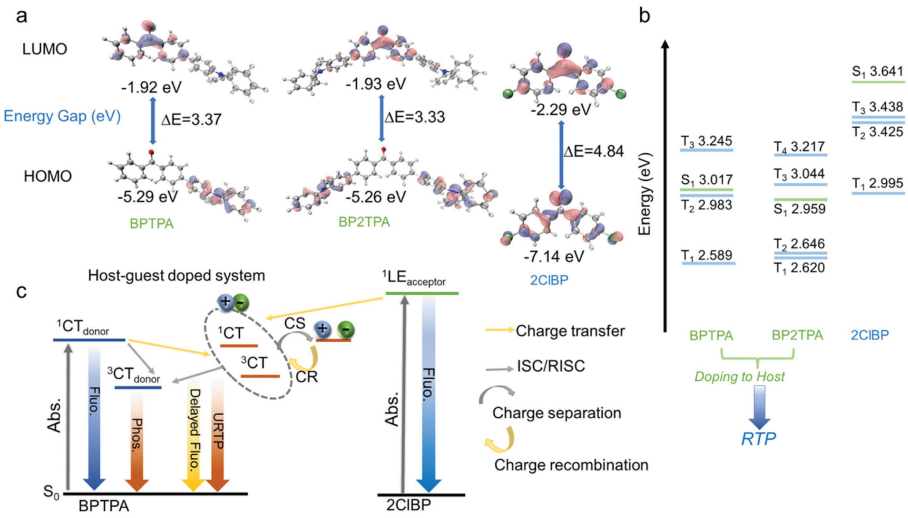

Fig. 2. (a) The HOMO and LUMO of guest and host molecules. (b) The energy levels of the BPTPA, BP2TPA and 2ClBP. (c) Proposed photophysical processes in the host-guest doped system.

spectra, as well as the photoluminescence spectra of the doping of the BPTPA/2ClBP doped at a molar ratio of 100:1 to form the nanosuspension. The results indicated that doping in the nanosuspension in the solvent does not significantly alter the emission spectra of the guest. It is worth noting that the doped system is clearly visible to the naked eye as a phosphorescence phenomenon at room temperature [2,43]. The difference is that for the BPTPA/2ClBP system, the emission intensity reaches a maximum when the water content is 90% and a clear RTP phenomenon can be observed. The BP2TPA/2ClBP polymerization has the highest emission intensity at 40% water content due to the greater steric hindrance of BP2TPA. Fig. S10 (Supporting information) shows the photoluminescence spectra of the two doped systems at 90% water content. The position of the phosphorescence emission peak is similar to that of the grinding doping. This suggests that this spontaneous aggregation can produce the same dynamic process as grinding doping. The apparent enhancement of the phosphorescence emission should also be associated with an improvement in the radiative attenuation of the exciton. Photophysical information about the host, guest and doped systems in the solid or solution state is summarized in Tables S1 and S2 (Supporting information).

Density functional theory (DFT) and time-dependent density functional theory (TDDFT) calculation were carried out to analyze molecular orbitals and excited state energy levels [44,45]. Meanwhile, Multiwfn program was used to analyze the frontier molecular orbital [46]. The specific calculation method is in the supporting information. Fig. 2a depicts that the highest occupied molecular orbital (HOMO) of BPTPA and BP2TPA is mainly located on triphenylamine, while the lowest unoccupied molecular orbital (LUMO) is located on benzophenone, which has obvious charge transfer (CT) characteristics. The electron density of HOMO and LUMO of 2ClBP is mainly located on benzophenone, which is an obvious local excitation (LE). It is similar to the experimental result, which confirms the reliability of the calculation. The value of the spin orbital coupling (SOC) constant of the single component (host/guest) is shown in Fig. S11 (Supporting information). It can be seen that individual guest molecules have small SOC values and therefore do not possess phosphorescent properties. Considering the synergistic effect of host and guest molecules in photoexcitation charge transfer, the singlet and triplet states energy levels of BPTPA, BP2TPA and 2ClBP were calculated (Fig. 2b). Combined with the analysis of the experimental data, the PL spectra of both doped systems have three distinct peaks with peaks located at approximately 480 nm, 550 nm and 600 nm. Meanwhile, the peak at 480 nm was confirmed to be the long-delayed fluorescence peak, while the peaks at 550 nm and 600 nm proved to be the URTP. Since BPTPA alone has been shown to exhibit shorter phosphorescence property. The ISC process occurs between the singlet and triplet states of BPTPA. And the host-guest doping produces a process of charge transfer separation-recombination from the donor (guest) and the acceptor (host) [10,47]. Further, this process induces a long-delayed fluorescence and URTP of the guest. BPTPA radical cation could be stable in the 2ClBP matrix. The corresponding photophysical processes are summarized in Fig. 2c.

To verify the URTP mechanism, we further investigated the excited state dynamics of URTP in the BPTPA/2ClBP doped system using transient absorption spectroscopy [48]. At an excitation wavelength of 355 nm, 2ClBP has no absorption peak at 400-700 nm (Fig. 3a). In contrast to the stimulated emission (SE) at 450-700 nm for BPTPA (Fig. 3b), the doped system exhibits a clear charge separation characteristic (Fig. 3c). During the 2 μs photoexcitation, the doped system shows a negative signal as a ground state bleaching (GSB) peak at ~410 nm. The SE signal at 450-500 nm corresponds to the fluorescence emission. Some reports mention that the positive signal of absorption in the transient absorption spectra of some long-lived CT systems correlates with the production of radical ions [12,49-51]. Therefore, as the SE signal diminished, two positive absorption peaks appeared at ~430 nm and ~550 nm, which were attributed to the charge separation generated by the radical ions $2ClBP^{-\cdot}$ and $BPTPA^{+\cdot}$. The collaborative interaction between host and guest is an integral factor in achieving URTP in the host-guest system.

Considering that the precise doped eutectic structure cannot be obtained, it will also be very limited in application. Therefore, we performed MD simulations in order to investigate the internal mechanism in depth [52]. The periodic cubic box was built, including a larger amount of the host 2ClBP with a smaller amount of the guest BPTPA. Considering the aggregation, the corresponding ratio is set to 50:1. We used the annealing process to simulate the heating process. Fig. S12 (Supporting information) shows the periodic annealing temperature procedure for the MD simulation. The statistical average density of the host and guest cubes during the simulation is 1.4 g/cm^3, which is consistent with the density of the host 2ClBP. After the MD process was completed, the cluster structure was further analyzed as shown in Fig. S13a (Supporting information). No obvious aggregation phenomenon was found,

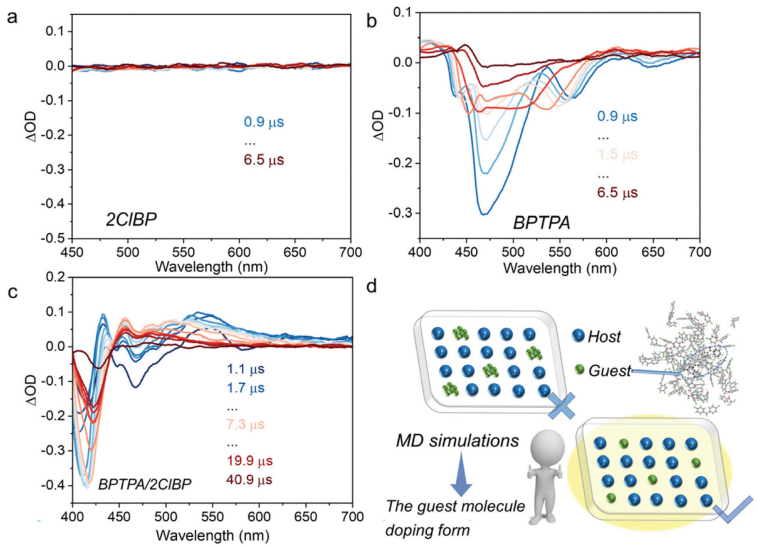

Fig. 3. Transient absorption spectra of (a) 2ClBP, (b) BPTPA and (c) BPTPA/2ClBP@1:100. Excitation wavelength: 355 nm. (d) Schematic of doping after MD simulation.

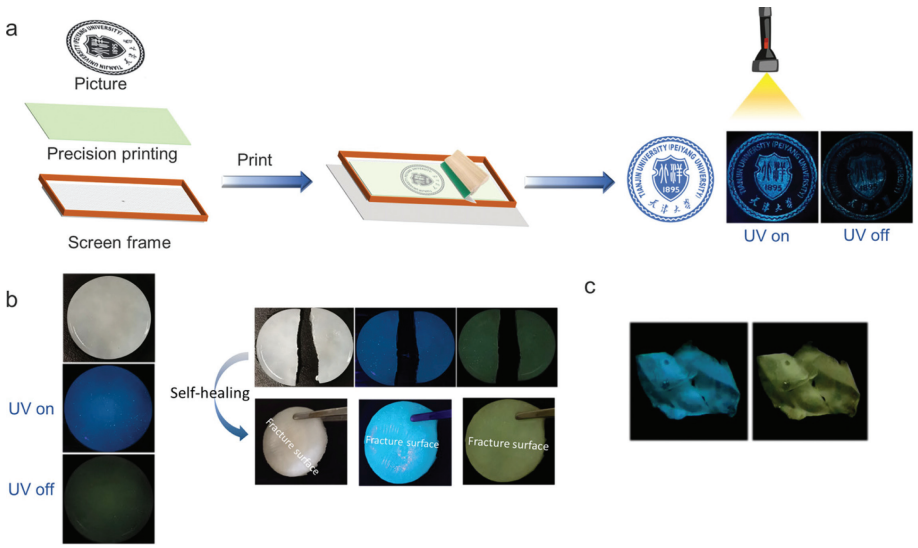

Fig. 4. (a) Screen printing application of doped system. (b) Doped system combined with PVA to realize self-healing. (c) Doped system combined with PVA to prepare flexible materials of different shapes.

so it does not prove that the guest molecules were doped into the host molecule in the form of aggregates (Fig. 3d). Then, we built a model based on the above simulated BPTPA/2ClBP and performed hybrid QM/MM calculations on this cluster using a two-layer ONIOM model to investigate the photophysical properties the dotted box in Fig. S13b (Supporting information). We calculated the conformational relaxation and geometric deviation, RMSD values, of the excited single and triplet state structures relative to the ground state structure. The average RMSD (S_1, S_0) and RMSD (T_1, S_0) of the guest in the host-guest system after MD simulations were calculated to be 0.178 and 0.128, which are much lower than the RMSD values of BPTPA under the isolated state calculation, corresponding to 0.331 and 0.749, indicating a limited vibration relaxation process (Figs. S13c and d in Supporting information). These results suggest that the rigid environment provided by the host can effectively reduce the non-radiative deactivation of the guest. From the above analysis, it can be concluded that 2ClBP can be a promising host substrate to suppress nonradiative losses by providing a robust environment for the guest.

After in-depth understanding of the mechanism, we demonstrated the potential applications of these host-guest systems. Since long URTP can be achieved by simple grinding or heating, these doped systems have great potential and can be used as some anti-counterfeiting materials, as shown in Fig. 4a, by screen printing technology. In addition, we can also consider combining with polyvinyl alcohol (PVA) to realize self-healing room temperature phosphorescence (Fig. 4b) [53]. Combining this property with the ease of cutting PVA films, we can prune phosphorescent doped films into any shape or pattern, greatly expanding the application in the field of flexible materials (Fig. 4c).

In conclusion, a novel organic host-guest doped system with excellent URTP performance has been developed with 2ClBP as the host and BPTPA and BP2TPA as the guests. The doped systems BPTPA/2ClBP@1:100 and BP2TPA/2ClBP@1:100 show a significant increase in phosphorescence quantum yield of 14.55% and 8.44% compared to the guest BPTPA and BP2TPA, respectively. The URTP lifetime can even be as long as ~270 ms. Different phosphor wavelengths correspond to different lifetimes, and different

photophysical processes are proposed. The charge transfer-separation-recombination process between the host and the guest is responsible for the realization of URTP, according to a combination of computational results and transient absorption spectra. The active role of the host in promoting the phosphorescence performance of the guest is analyzed by detailed experiments combined with molecular dynamics simulations. Finally, the application of the doped system in the field of flexible materials is extended. This work helps to establish a new doping system. In terms of design strategy, URTP is achieved by introducing carbonyl groups with lone pair electrons, similar structure of host and guest parts, favourable host and guest energy levels, charge transfer-separation-recombination. Therefore, it provides important guidance for some potential phosphorescent molecules.

Declaration of competing interest

The authors declare that they have no known competing financial interests or personal relationships that could have appeared to influence the work reported in this paper.

Acknowledgments

This work was supported by the National Natural Science Foundation of China (Nos. 21873068, 21573229 and 21422309). Guangjiu Zhao also thanks the financial support from Double First-Rate and Peiyang Scholar Projects (Tianjin University), the Open Research Funds of State Key Laboratory of Bioelectronics (Southeast University), the Frontier Science Project of the Knowledge Innovation Program of Chinese Academy of Sciences (CAS).

Supplementary materials

Supplementary material associated with this article can be found, in the online version, at doi:10.1016/j.cclet.2022.108062.

References

[1] S. Cai, H. Shi, J. Li, et al., Adv. Mater. 29 (2017) 1701244.
[2] Y. Wang, H. Gao, J. Yang, et al., Adv. Mater. 33 (2021) 2007811.
[3] P. Xue, P. Wang, P. Chen, et al., Chem. Sci. 8 (2017) 6060–6065.
[4] Y. Deng, D. Zhao, X. Chen, et al., Chem. Commun. 49 (2013) 5751–5753.
[5] Z. Yang, Z. Mao, X. Zhang, et al., Angew. Chem. Int. Ed. 55 (2016) 2181–2185.
[6] H. Feng, J. Zeng, P. Yin, et al., Nat. Commun. 11 (2020) 2617.
[7] J. Lee, H.F. Chen, T. Batagoda, et al., Nat. Mater. 15 (2016) 92–98.
[8] M. Kim, S.K. Jeon, S.H. Hwang, J.Y. Lee, Adv. Mater. 27 (2015) 2515–2520.
[9] B. Wu, N. Guo, X. Xu, et al., Adv. Opt. Mater. 8 (2020) 2001192.
[10] Z. Lin, R. Kabe, K. Wang, C. Adachi, Nat. Commun. 11 (2020) 191.
[11] K. Jinnai, R. Kabe, Z. Lin, C. Adachi, Nat. Mater. 21 (2021) 338–344.
[12] R. Kabe, C. Adachi, Nature 550 (2017) 384–387.
[13] S. Kuila, S.J. George, Angew. Chem. Int. Ed. 59 (2020) 9393–9397.
[14] A.M. Messinis, A.S. Batsanov, W.R.H. Wright, et al., ACS Catal. 8 (2018) 11249–11263.
[15] S. Guo, W. Dai, X. Chen, et al., ACS Mater. Lett. 3 (2021) 379–397.
[16] Y. Wen, H. Liu, S. Zhang, et al., J. Mater. Chem. C 7 (2019) 12502–12508.
[17] Z. Yang, C. Xu, W. Li, et al., Angew. Chem. Int. Ed. 59 (2020) 17451–17455.
[18] J. Wei, B. Liang, R. Duan, et al., Angew. Chem. Int. Ed. 55 (2016) 15589–15593.
[19] P. Pander, A. Swist, R. Turczyn, et al., J. Phys. Chem. C 122 (2018) 24958–24966.
[20] Z. An, C. Zheng, Y. Tao, et al., Nat. Mater. 14 (2015) 685–690.
[21] L. Xu, G. Li, T. Xu, et al., Chem. Commun. 54 (2018) 9226–9229.
[22] G. Zhang, J. Chen, S.J. Payne, et al., J. Am. Chem. Soc. 129 (2007) 8942–8943.
[23] H. Chen, X. Yao, X. Ma, H. Tian, Adv. Opt. Mater. 4 (2016) 1397–1401.
[24] L. Gu, H. Wu, H. Ma, et al., Nat. Commun. 11 (2020) 944.
[25] Y. Tian, J. Yang, Z. Liu, et al., Angew. Chem. Int. Ed. 60 (2021) 20259–20263.
[26] X. Liu, Y. Pan, Y. Lei, et al., J. Phys. Chem. Lett. 12 (2021) 7357–7364.
[27] Y. Chen, Y. Xie, H. Shen, et al., Chem. Eur. J. 26 (2020) 17376–17380.
[28] Y. Lei, J. Yang, W. Dai, et al., Chem. Sci. 12 (2021) 6518–6625.
[29] X. Zhang, L. Du, W. Zhao, et al., Nat. Commun. 10 (2019) 5161.
[30] X. Liu, W. Dai, J. Qian, et al., J. Mater. Chem. C 9 (2021) 3391–3395.
[31] Y. Lei, W. Dai, J. Guan, et al., Angew. Chem. Int. Ed. 59 (2020) 16054–16060.
[32] S. Hirata, K. Totani, J. Zhang, et al., Adv. Funct. Mater. 23 (2013) 3386–3397.
[33] M.S. Kwon, D. Lee, S. Seo, J. Jung, J. Kim, Angew. Chem. Int. Ed. 53 (2014) 11177–11181.
[34] B. Ding, L. Ma, Z. Huang, X. Ma, H. Tian, Sci. Adv. 7 (2021) eabf9668.
[35] Y. Zhao, B. Ding, Z. Huang, X. Ma, Chem. Sci. 13 (2022) 8412–8416.
[36] L. Ma, Q. Xu, S. Sun, et al., Angew. Chem. Int. Ed. 61 (2022) e202115748.
[37] H. Gui, Z. Huang, Z. Yuang, X. Ma, CCS Chem. 4 (2022) 173–181.
[38] Y. Pan, J. Li, X. Wang, et al., Adv. Funct. Mater. 32 (2022) 2110207.
[39] Y. Sun, G. Wang, X. Li, B. Zhou, K. Zhang, Adv. Opt. Mater. 9 (2021) 2100353.
[40] Y. Sun, J. Liu, J. Li, et al., Adv. Opt. Mater. 10 (2022) 2101909.
[41] W. Yuan, X. Shen, H. Zhao, et al., J. Phys. Chem. C 114 (2010) 6090–6099.
[42] W. Luo, Y. Zhang, Y. Gong, et al., Chin. Chem. Lett. 29 (2018) 1533–1536.
[43] F. Xiao, H. Gao, Y. Lei, et al., Nat. Commun. 13 (2022) 186.
[44] C. Lee, W. Yang, R.G. Parr, Phys. Rev. B 37 (1988) 785–789.
[45] M.J. Frisch, G.W. Trucks, H.B. Schlegel, et al., Gaussian 16 Rev. C.01, Wallingford, CT (2016).
[46] T. Lu, F. Chen, J. Comput. Chem. 33 (2012) 580–592.
[47] Z. Lin, R. Kabe, N. Nishimura, K. Jinnai, C. Adachi, Adv. Mater. 30 (2018) 1803713.
[48] D. Liu, A.M. El-Zohry, M. Taddei, et al., Angew. Chem. Int. Ed. 59 (2020) 11591–11599.
[49] C. Chen, Z. Chi, K.C. Chong, et al., Nat. Mater. 20 (2021) 175–180.
[50] X. Chen, A.A. Sukhanov. Y. Yan, et al., Angew. Chem. Int. Ed. 61 (2022) e202203758.
[51] Y. Dong, A. Elmali, J. Zhao, B. Dick, A. Karatay, ChemPhysChem 21 (2020) 1388–1401.
[52] M. Li, X. Cai, Z. Chen, et al., Chem. Sci. 12 (2021) 13580.
[53] D. Lee, O. Bolton, B.C. Kim, et al., J. Am. Chem. Soc. 135 (2013) 6325–6329.